An Unusual Near-Eclipsed Porphyrin Ring Orientation in Two Crystalline Forms of mu-Oxo)bis[(octaethylporphinato)iron(III)]. Structural and Molecular Mechanics Studies

ARTICLE *in* INORGANIC CHEMISTRY · JANUARY 1995

Impact Factor: 4.76

CITATIONS
19

READS
12

6 AUTHORS, INCLUDING:

Jonah Erlebacher
Johns Hopkins University
84 PUBLICATIONS **5,045** CITATIONS
SEE PROFILE

John A Shelnutt
University of Georgia
265 PUBLICATIONS **8,867** CITATIONS
SEE PROFILE

W. Robert Scheidt
University of Notre Dame
363 PUBLICATIONS **13,757** CITATIONS
SEE PROFILE

An Unusual Near-Eclipsed Porphyrin Ring Orientation in Two Crystalline Forms of (μ-Oxo)bis[(octaethylporphinato)iron(III)]. Structural and Molecular Mechanics Studies

Beisong Cheng,[1a] J. David Hobbs,[1b] Peter G. Debrunner,[1c] Jonah Erlebacher,[1d] John A. Shelnutt,*[,1b] and W. Robert Scheidt*[,1a]

Department of Chemistry and Biochemistry, University of Notre Dame, Notre Dame, Indiana 46556, Department of Physics, University of Illinois, Urbana, Illinois 61801, Sandia National Laboratory, Albuquerque, New Mexico 87185, and Institute for Cancer Research, Fox Chase Cancer Center, Philadelphia, Pennsylvania 19111

Received July 1, 1994[⊗]

The structures of two polymorphs of (μ-oxo)bis[(octaethylporphinato)iron(III)], $[Fe(OEP)]_2O$ ($C_{72}H_{88}Fe_2N_8O$), have been determined by X-ray structure analyses using data collected with an area detector. The two $[Fe(OEP)]_2O$ polymorphs (a triclinic and a monoclinic form) show strong structural similarities. The eight $Fe-N_p$ bond distances have average values of 2.077(3) Å in the triclinic form and 2.080(5) Å in the monoclinic form. The average axial Fe−O bond lengths are 1.756(3) and 1.755(10) Å for the two structures, respectively. The average displacements of the iron(III) atom from the mean porphinato core are 0.50 Å in the triclinic form and 0.54 Å in the monoclinic form. The most important structural feature of the molecule in the two crystal forms is the near-eclipsed intramolecular porphyrin ring orientation: the average N−Fe−Fe′−N′ dihedral angles are 17.0(10)° in the triclinic form and 16.8(6)° in the monoclinic form. Molecular mechanics calculations have been carried out to explore the inter-ring orientation; these suggest that peripheral ethyl group interactions lead to the near-eclipsed orientation. Crystal data: triclinic form, $a = 11.561(5)$ Å, $b = 12.299(8)$ Å, $c = 23.341(16)$ Å, $\alpha = 82.56(3)°$, $\beta = 81.94(7)°$, $\gamma = 79.18(1)°$, space group $P\bar{1}$, $V = 3210(5)$ Å^3, $Z = 2$, 8931 observed data, $R_1 = 0.050$, $R_2 = 0.056$; monoclinic form, $a = 18.433(13)$ Å, $b = 15.104(6)$ Å, $c = 23.489(6)$ Å, $\beta = 97.82(1)°$, space group $P2_1/c$, $V = 6479(9)$ Å^3, $Z = 4$, 6169 observed data, $R_1 = 0.054$, $R_2 = 0.060$.

Introduction

We recently reported[2] the synthesis, molecular structure, and preliminary magnetic characterization of the novel μ-hydroxo bridged compound $\{[Fe(OEP)]_2(OH)\}ClO_4$.[3] One unexpected feature of the molecular structure is the fact that the two intramolecular porphyrin rings are nearly eclipsed with an average N−Fe−Fe′−N′ dihedral angle (twist angle) of only 8.4°. We thought that inter-ring interactions, especially those involving the peripheral ethyl groups, are probably responsible for the near-eclipsing of the two octaethylporphyrinato rings. The inter-ring interactions in this molecule are accentuated by their nonparallel orientation; their probable importance is underscored by the fact that the angle (146.2°) is 20−30° larger than might be expected for a μ-hydroxo ligand.[4] These observations led us to undertake the structural study of the analogous $[Fe(OEP)]_2O$ complex to further examine these inter-ring interactions.

During the course of this study we obtained two crystalline forms of $[Fe(OEP)]_2O$, one triclinic and one monoclinic, and we determined the molecular structures of both. The molecular structure of both show the strong similarities that would be expected if inter-ring interactions are an important facet of their stereochemistry. During the course of this work we also learned that the structure of the triclinic crystal form of $[Fe(OEP)]_2O$ had been independently obtained at the Institute for Cancer Research (Fox Chase); their structural results differ immaterially from our structure determination. In addition to the structure determinations, we used molecular mechanics calculations to probe the importance of the peripheral groups in defining the porphyrin inter-ring orientation; these calculations confirm the importance of the peripheral groups.

As reported in this paper, our molecular mechanics calculations confirm that the near-eclipsed orientation of the two porphinato rings in each derivative is primarily the result of peripheral ethyl group interactions. These conclusions are wholly consistent with recent work on μ-oxo macrocyclic derivatives related to porphyrins.

Experimental Section

General Information. H_2OEP was purchased from Midcentury Chemicals; dichloromethane, hexanes, ferrous chloride and potassium hydroxide were purchased from Fisher. All materials were used as received, except $FeCl_2$, which was dried under vacuum (~190 °C) before use. IR spectra were determined as KBr pellets on a Perkin-Elmer 883 spectrometer. The Mössbauer sample was an Apiezon N grease suspension of finely ground crystals. As noted below, at least some crystalline preparations contain two different polymorphs. We have no easy way to distinguish the two polymorphs and no method to selectively crystallize either form. Thus, both crystalline forms might have been included in the Mössbauer sample. Measurements were performed on a constant-acceleration spectrometer, and isomer shifts are quoted relative to iron metal at 300 K.

Synthesis and Characterization of $[Fe(OEP)]_2O$. $[Fe(OEP)]_2O$ was prepared from [Fe(OEP)Cl][5] by literature methods.[6] In a typical

⊗ Abstract published in *Advance ACS Abstracts,* November 15, 1994.

(1) (a) University of Notre Dame. (b) Sandia National Laboratory. (c) University of Illinois. (d) Institute for Cancer Research.

(2) Scheidt, W. R.; Cheng, B.; Safo, M. K.; Cukiernik, F.; Marchon, J.-C.; Debrunner, P. G. *J. Am. Chem. Soc.* **1992**, *114*, 4420.

(3) Abbreviations used in this paper: OEP, octaethylporphyrin dianion; TPP, 5,10,15,20-tetraphenylporphyrin dianion; TF_5PP, 5,10,15,20-tetrakis(pentafluorophenyl)porphyrin dianion; TMPyP, 5,10,15,20-tetrakis(1-methylpyridinium-4-yl)porphyrin dianion; NCH_3TPP, *N*-methyl-*meso*-tetraphenylporphyrin monoanion; TPC, 5,10,15,20-tetraphenylchlorin dianion; ODM, 5,15-dimethyl-2,3,7,8,12,13,17,18-octaethylporphyrin dianion; FF, face-to-face porphyrin dianion; Pc, phthalocyanine dianion; TPrPc, 2,7,12,17-tetra-*n*-propylporphycene dianion; TBuPc, 2,7,12,17-tetra-*tert*-butylporphycene dianion; N_p, porphinato nitrogen atom; Ct, center of the porphyrin ring.

(4) Kurtz, D. M., Jr. *Chem. Rev.* **1990**, *90*, 585.

0020-1669/95/1334-0102$09.00/0

preparation, a 25 mL dichloromethane solution of [Fe(OEP)Cl] (~1.0 g) was vigorously shaken in a separatory funnel with 250 mL of aqueous KOH solution (~2 M) and then washed with distilled water. The dichloromethane layer was separated from the mixture and dried with Na_2SO_4, and the product was washed out of the Na_2SO_4 with CH_2Cl_2 on a fritted glass filter. The filtrate was then evacuated to dryness, and $[Fe(OEP)]_2O$ was collected as a microcrystalline sample. X-ray quality crystals were prepared by dissolving 30 mg in 1.5 mL of CH_2Cl_2 and allowing hexanes to diffuse into the solution. After about 1 week, black platelike crystals of $[Fe(OEP)]_2O$ were isolated, from which two polymorphs of the compound were identified by single-crystal X-ray crystallography. IR: 877 cm^{-1} (s), Fe−O−Fe asymmetric stretch.

X-ray Structure Determinations.[7] The X-ray analyses of the two polymorphs were done on an Enraf-Nonius FAST area-detector diffractometer with a Mo rotating-anode source (λ = 0.710 73 Å). Our detailed methods and procedures for small-molecule X-ray data collection with the FAST system have been described.[8] Data were corrected for Lorentz and polarization factors but not for absorption. We estimate that the errors in F resulting from neglect of absorption are no greater than ±4% for triclinic $[Fe(OEP)]_2O$ and no greater than ±3% for the monoclinic form. Moreover, absorption effects were further reduced when the four partial data sets, collected at different crystal orientations, were merged and rescaled. A brief summary of crystal data and data collection parameters is listed in Table 1, and the complete crystallographic details are included in the supplementary material.

The two structures were solved by using the direct methods program MULTAN (~25% of the heavy atoms found); the remaining non-hydrogen atoms were located by difference Fourier syntheses. All porphyrin hydrogen atoms were idealized (C−H = 0.95 Å, B(H) = B(C) × 1.2) and included in subsequent least-squares refinement as fixed contributors. The final least-squares refinement with anisotropic thermal parameters for all the non-hydrogen atoms led to discrepancy indices of R_1 = 0.050, R_2 = 0.056 with 8931 observed data ($F_o \geq 2.0\sigma(F_o)$) for the triclinic form and R_1 = 0.054, R_2 = 0.060 with 6169 observed data for the monoclinic form. Atomic coordinates for the two structures are presented in Table 2. Anisotropic thermal parameters and the fixed hydrogen atom coordinates for both structures are included in the supplementary material.

Molecular Mechanics Calculations. Energy optimized porphyrin structures were determined using Cerius[2] (Version 1.1) software (Molecular Simulation, Inc.) with a force field that is based upon potential energy functions described previously and force constants obtained from a recent normal-coordinate analysis of Ni(OEP).[9] The development of the force field has been described in detail elsewhere.[10] In subsequent work,[11] the following changes were implemented: (1) electrostatic terms were included in calculating the total energy, (2) the van der Waals potential energy term for the hydrogen atoms was changed from a Lennard−Jones 6−12 to an exponential (r^{-6}) functional form, and (3) a cutoff distance of 50 Å was employed in calculation of electrostatic and van der Waals potential energy terms. These changes did not significantly affect the calculated structures, but did alter the ordering of the optimized energies for the various conformers possible as a result of different initial ethyl group orientations. Partial atomic charges used in determining the contribution of the electristatic energy to the total energy were calculated using the charge equilibration method of Rappé and Goddard.[12] Electrostatic charges were updated periodically during the energy minimizations using this method. Finally, in the calculation of these porphyrin dimer structures, a new atom type for the oxygen atom bound by two iron atoms was created. Thus, two new potential energy terms, one for the Fe−O bond stretch and the other for the Fe−O−Fe angle bend, were introduced in the force field. The parameters for these terms are summarized in Table S8 of the supplementary material. For this series of calculations, the following procedure was employed: Single molecules of the two crystal forms of $[Fe(OEP)]_2O$ were extracted from the crystal lattice built from the cell parameters and atomic coordinates. The molecules were then relaxed by running 1 ps of quenched dynamics at 300 K. The Fe−O bonds and Fe−O−Fe angle were then optimized by a conjugate-gradient method of energy minimization. The dimers were then allowed to minimize until the rms forces were less than or equal to 0.001 kcal mol^{-1} $Å^{-1}$.

Table 1. Crystallographic Data for the Two Crystal Forms of $[Fe(OEP)]_2O$

	triclinic	monoclinic
formula	$C_{72}H_{88}Fe_2N_8O$	$C_{72}H_{88}Fe_2N_8O$
fw	1193.24	1193.24
a, Å	11.561(5)	18.433(13)
b, Å	12.299(8)	15.104(6)
c, Å	23.341(16)	23.489(6)
α, deg	82.56(3)	90.00
β, deg	81.94(7)	97.82(1)
γ, deg	79.18(1)	90.00
V, Å^3	3210(5)	6479(9)
Z	2	4
space group	$P\bar{1}$ (No. 2)	$P2_1/c$ (No. 14)
T, °C	20(1)	20(1)
λ, Å	0.710 73	0.710 73
ϱ_{calc}, g/cm^3	1.235	1.223
μ, cm^{-1}	4.985	4.939
R_1[a]	0.050	0.054
R_2[b]	0.056	0.060

[a] $R_1 = \sum||F_o| - |F_c||/\sum|F_o|$. [b] $R_2 = [\sum w(|F_o| - |F_c|)^2/\sum w(F_o)^2]^{1/2}$.

Results

Molecular Structures. ORTEP diagrams of triclinic $[Fe(OEP)]_2O$ are shown in Figures 1 and 2. Figure 2 also illustrates the labeling scheme used in the tables for the non-hydrogen atoms. For ring 2, since the nomenclature of the atoms is exactly the same as that in ring 1, only the four pyrrole nitrogen atoms are labeled. In all tables, the atom names of ring 1 are preceded by the numeral "1" and those of ring 2 by

(5) Buchler, J. W. In *Porphyrins and Metalloporphyrins*; Smith, K. M., Ed.; Elsevier Scientific Publishing: Amsterdam, 1975; Chapter 5.
(6) (a) Sadasivan, N.; Eberspaecher, H. I.; Fuchsman, W. H.; Caughey, W. S. *Biochemistry* **1969**, *8*, 534. (b) La Mar, G. N.; Eaton, G. R.; Holm, R. H.; Walker, F. A. *J. Am. Chem. Soc.* **1973**, *95*, 63. (c) O'Keeffe, D. H.; Barlow, C. H.; Smythe, G. A.; Fuchsman, W. H.; Moss, T. H.; Lilienthal, H. R.; Caughey, W. S. *Bioinorg. Chem.* **1975**, 125.
(7) Programs used in this study include the following. (a) MADNES routines used in FAST data collection and reduction (J. W. Pflugrath, Cold Spring Harbor, and A. Messerschmidt, Max-Plank-Institute für Biochemie, Martinsried, unpublished). (b) The program ABSURD used in data abstraction (I. Tickle, Birbeck College, and P. Evans, MRC, unpublished). (c) The program SCALEXPRO used in averaging and rescaling of data sets (H. L. Carrell, The Institute for Cancer Research, Fox Chase Cancer Center). (d) Direct methods program MULTAN: Main, P.; Hull, S. E.; Lessinger, L.; Germain, G.; Declerq, J.-P.; Woolfson, M. M. *MULTAN*, a system of computer programs for the automatic solution of crystal structures from X-ray diffraction data. Universities of York, U.K., and Louvain, Belgium. (e) Zalkin's FORDAP for difference Fourier syntheses. (f) Local modified least-squares refinement: Lapp, R. L.; Jacobson, R. A. ALLS, a generalized crystallographic least-squares program. National Technical Information Services, Springfield, VA (IS-4708 UC-4). (g) Busing and Levy's ORFFE and ORFLS and Johnson's ORTEP2. (h) Atomic form factors from: Cromer, D. T.; Mann, J. B. *Acta Crystallogr., Sect. A* **1968**, *24*, 321. Real and imaginary corrections for anomalous dispersion in the form factor of the iron and chlorine atoms from: Cromer, D. T.; Liberman, D. J. *J. Chem. Phys.* **1970**, *53*, 1891. Scattering factors for hydrogen from: Stewart, R. F.; Davidson, E. R.; Simpson, W. T. *J. Chem. Phys.* **1965**, *42*, 3175.
(8) Scheidt, W. R.; Turowska-Tyrk, I. *Inorg. Chem.* **1994**, *33*, 1314.
(9) (a) Li, X.-Y.; Czernuszewicz, R. S.; Kincaid, J. R.; Stein, P.; Spiro, T. G. *J. Phys. Chem.* **1990**, *94*, 47. (b) Li, X.-Y.; Czernuszewicz, R. S.; Kincaid, J. R.; Stein, P.; Spiro, T. G. *J. Am. Chem. Soc.* **1989**, *111*, 7012.
(10) (a) Shelnutt, J. A.; Medforth, C. J.; Berber, M. D.; Barkigia, K. M.; Smith, K. M. *J. Am. Chem. Soc.* **1991**, *113*, 4077. (b) Sparks, L. D.; Medforth, C. J.; Park, M.-S.; Chamberlain, J. R.; Ondrias, M. R.; Senge, M. O.; Smith, K. M.; Shelnutt, J. A. *J. Am. Chem. Soc.* **1993**, *115*, 581.
(11) Hobbs, J. D.; Medforth, C. J.; Majumder, S. A.; Luo, L.; Quirke, J. M.; Shelnutt, J. A. *J. Am. Chem. Soc.* **1994**, *116*, 3261.
(12) Rappé, A. K.; Goddard, W. A., III. *J. Phys. Chem.* **1991**, *95*, 3358.

Table 2. Fractional Coordinates of $[Fe(OEP)]_2O$[a]

	triclinic				monoclinic			
atom	*x*	*y*	*z*	B_{eq}[b]	*x*	*y*	*z*	B_{eq}[b]
Fe(1)	0.32069(4)	0.82534(4)	0.227315(20)	2.57	0.32482(4)	1.00255(6)	0.255519(26)	2.69
Fe(2)	0.14328(4)	0.62109(4)	0.272586(20)	2.48	0.13454(4)	1.00148(5)	0.214766(25)	2.42
O	0.23212(24)	0.72138(21)	0.24501(11)	3.3	0.22884(19)	1.00187(25)	0.23746(15)	3.7
1N(1)	0.48990(25)	0.73521(24)	0.23360(12)	3.0	0.35278(25)	1.13561(27)	0.24853(18)	3.0
1N(2)	0.36382(27)	0.83565(24)	0.13752(12)	3.0	0.34327(25)	1.02064(26)	0.34418(17)	3.1
1N(3)	0.20043(26)	0.97117(23)	0.21294(12)	2.9	0.36091(24)	0.86976(27)	0.27232(18)	2.9
1N(4)	0.32696(28)	0.87161(25)	0.30917(12)	3.2	0.36126(25)	0.98465(27)	0.17661(17)	3.3
2N(1)	0.25745(26)	0.47029(24)	0.26426(12)	2.9	0.10556(27)	1.13375(27)	0.22236(18)	3.0
2N(2)	0.08126(26)	0.59696(24)	0.19675(12)	2.9	0.09201(24)	0.98127(25)	0.29143(17)	2.9
2N(3)	−0.02213(25)	0.71542(25)	0.29449(12)	3.0	0.10936(24)	0.86974(26)	0.19587(17)	2.7
2N(4)	0.15611(25)	0.59155(23)	0.36160(11)	2.8	0.12274(23)	1.02173(24)	0.12670(16)	2.6
1C(a1)	0.5398(3)	0.6982(3)	0.28404(17)	3.5	0.3621(3)	1.1789(4)	0.19883(24)	3.5
1C(a2)	0.5585(3)	0.6758(3)	0.19133(16)	3.4	0.3515(3)	1.1986(3)	0.28991(24)	3.3
1C(a3)	0.4506(3)	0.7633(3)	0.10808(15)	3.3	0.3414(4)	1.0998(4)	0.37211(24)	3.6
1C(a4)	0.2961(3)	0.8943(3)	0.09629(15)	3.3	0.3405(3)	0.9557(4)	0.38519(23)	3.6
1C(a5)	0.1551(3)	1.0132(3)	0.16169(16)	3.3	0.3472(3)	0.8255(3)	0.32234(23)	3.2
1C(a6)	0.1347(3)	1.0332(3)	0.25476(16)	3.4	0.3589(3)	0.8067(4)	0.23159(24)	3.4
1C(a7)	0.2373(4)	0.9400(3)	0.33848(16)	3.7	0.3649(4)	0.9045(4)	0.14918(24)	3.8
1C(a8)	0.3950(4)	0.8136(3)	0.34976(16)	3.7	0.3684(4)	1.0489(4)	0.13686(25)	4.1
2C(a1)	0.3303(3)	0.4136(3)	0.30397(15)	3.1	0.1126(3)	1.1986(3)	0.18191(24)	3.3
2C(a2)	0.2924(3)	0.42006(29)	0.21393(16)	3.2	0.0970(3)	1.1764(4)	0.27214(24)	3.5
2C(a3)	0.1445(3)	0.53590(29)	0.15384(15)	3.1	0.0854(3)	1.0439(4)	0.33245(22)	3.2
2C(a4)	−0.0079(3)	0.6675(3)	0.17107(15)	3.2	0.0870(3)	0.9013(4)	0.31787(23)	3.2
2C(a5)	−0.1013(3)	0.7657(3)	0.25642(16)	3.2	0.1001(3)	0.8045(3)	0.23451(23)	3.3
2C(a6)	−0.0622(3)	0.7611(3)	0.34592(15)	3.1	0.1166(3)	0.8267(3)	0.14528(22)	3.0
2C(a7)	0.0947(3)	0.65537(29)	0.40345(14)	2.9	0.1285(3)	0.9592(3)	0.08493(22)	3.1
2C(a8)	0.2456(3)	0.5219(3)	0.38712(15)	3.1	0.1274(3)	1.1023(3)	0.10028(21)	2.9
1C(b1)	0.6450(4)	0.6149(3)	0.27271(19)	4.0	0.3673(3)	1.2738(4)	0.20989(26)	3.6
1C(b2)	0.6547(4)	0.6002(3)	0.21553(18)	3.9	0.3606(4)	1.2860(4)	0.26579(27)	3.8
1C(b3)	0.4357(4)	0.7768(3)	0.04700(16)	3.8	0.3379(4)	1.0851(4)	0.43235(26)	4.3
1C(b4)	0.3407(4)	0.8580(3)	0.03955(16)	3.8	0.3372(4)	0.9955(5)	0.44045(22)	4.2
1C(b5)	0.0565(4)	1.1043(3)	0.17217(17)	3.8	0.3532(3)	0.7306(4)	0.31289(25)	3.7
1C(b6)	0.0469(3)	1.1181(3)	0.22948(17)	3.6	0.3607(3)	0.7192(4)	0.25774(25)	3.4
1C(b7)	0.2479(4)	0.9226(4)	0.40015(17)	4.4	0.3759(6)	0.9199(4)	0.09065(28)	5.3
1C(b8)	0.3453(4)	0.8448(4)	0.40723(18)	4.5	0.3780(5)	1.0093(5)	0.08295(25)	5.3
2C(b1)	0.4134(3)	0.3247(3)	0.27774(16)	3.3	0.1071(4)	1.2854(4)	0.20846(27)	3.8
2C(b2)	0.3898(3)	0.32902(29)	0.22228(16)	3.3	0.0970(4)	1.2712(3)	0.26334(25)	3.7
2C(b3)	0.0936(4)	0.5687(3)	0.10002(16)	3.4	0.07478(27)	1.0021(4)	0.38580(21)	3.5
2C(b4)	−0.0003(4)	0.6501(3)	0.11057(16)	3.5	0.0767(3)	0.9137(4)	0.37677(23)	3.5
2C(b5)	−0.1942(3)	0.8435(3)	0.28398(17)	3.5	0.1013(3)	0.7187(4)	0.20795(25)	3.3
2C(b6)	−0.1702(3)	0.8409(3)	0.33978(16)	3.4	0.1115(3)	0.7315(3)	0.15333(23)	3.4
2C(b7)	0.1478(3)	0.6260(3)	0.45734(15)	3.1	0.13582(27)	1.0009(4)	0.03083(19)	3.1
2C(b8)	0.2426(3)	0.5432(3)	0.44695(15)	3.3	0.1354(3)	1.0896(4)	0.04016(22)	3.3
1C(m1)	0.4949(4)	0.7344(4)	0.33766(17)	4.0	0.3678(4)	1.1389(4)	0.14729(24)	4.0
1C(m2)	0.5386(3)	0.6894(3)	0.13398(17)	3.6	0.3446(4)	1.1822(4)	0.34636(25)	4.0
1C(m3)	0.1989(4)	0.9756(3)	0.10855(16)	3.5	0.3411(4)	0.8658(4)	0.37402(25)	4.0
1C(m4)	0.1504(4)	1.0151(3)	0.31270(17)	3.8	0.3630(4)	0.8236(4)	0.17491(24)	3.9
2C(m1)	0.3262(3)	0.4402(3)	0.36006(15)	3.1	0.1226(3)	1.1830(3)	0.12593(23)	3.3
2C(m2)	0.2414(3)	0.4536(3)	0.16269(15)	3.3	0.0881(4)	1.1345(4)	0.32302(24)	3.6
2C(m3)	−0.0927(3)	0.7432(3)	0.19929(16)	3.5	0.0903(4)	0.8201(3)	0.29042(25)	3.6
2C(m4)	−0.0060(3)	0.7336(3)	0.39554(14)	3.1	0.1257(3)	0.8685(3)	0.09411(21)	2.9
1C(11)	0.7257(4)	0.5572(4)	0.31716(20)	4.8	0.3808(4)	1.3427(4)	0.16618(27)	4.6
1C(21)	0.7441(4)	0.5177(4)	0.18230(19)	4.3	0.3651(4)	1.3711(4)	0.29919(29)	4.7
1C(31)	0.5132(5)	0.7102(4)	0.00205(18)	4.9	0.3353(5)	1.1580(5)	0.4772(3)	6.0
1C(41)	0.2912(5)	0.9037(4)	−0.01672(18)	4.7	0.3343(5)	0.9471(5)	0.49630(28)	5.4
1C(51)	−0.0174(4)	1.1694(4)	0.12701(19)	4.7	0.3514(4)	0.6614(4)	0.35841(28)	5.0
1C(61)	−0.0348(4)	1.2071(4)	0.26176(19)	4.3	0.3754(4)	0.6351(4)	0.22742(26)	4.2
1C(71)	0.1594(5)	0.9803(5)	0.44667(20)	5.8	0.4012(6)	0.8391(7)	0.0472(3)	7.4
1C(81)	0.3914(5)	0.7932(5)	0.46513(22)	5.7	0.4017(5)	1.0589(5)	0.0260(4)	7.3
2C(11)	0.5019(4)	0.2417(4)	0.30933(18)	4.1	0.1116(4)	1.3715(4)	0.17662(27)	4.4
2C(21)	0.4479(4)	0.2524(3)	0.17740(18)	3.9	0.0889(4)	1.3399(4)	0.30794(25)	4.9
2C(31)	0.1430(4)	0.5244(4)	0.04303(17)	4.3	0.0675(4)	1.0489(4)	0.44107(25)	4.3
2C(41)	−0.0793(4)	0.7186(4)	0.06851(18)	4.3	0.0728(4)	0.8405(4)	0.41915(26)	4.2
2C(51)	−0.2932(4)	0.9150(4)	0.25442(19)	4.3	0.0960(4)	0.6323(4)	0.24030(27)	4.2
2C(61)	−0.2395(4)	0.9086(4)	0.38568(17)	4.0	0.1193(4)	0.6634(4)	0.10822(25)	4.0
2C(71)	0.1034(4)	0.6750(3)	0.51362(16)	3.7	0.1415(4)	0.9546(4)	−0.02453(24)	3.8
2C(81)	0.3250(4)	0.4806(4)	0.44837(17)	3.9	0.1391(4)	1.1624(4)	−0.00232(24)	3.9
1C(12)	0.6894(6)	0.4530(5)	0.34642(24)	6.9	0.4612(5)	1.3555(5)	0.1623(4)	6.6
1C(22)	0.6938(5)	0.4179(4)	0.17461(23)	5.7	0.4389(5)	1.3898(6)	0.3295(4)	7.6
1C(32)	0.6254(5)	0.7493(5)	−0.01807(24)	6.5	0.4083(6)	1.1887(6)	0.4969(4)	8.5
1C(42)	0.3511(6)	0.9906(6)	−0.05110(26)	8.0	0.4072(6)	0.9295(7)	0.5268(4)	9.1
1C(52)	0.0279(6)	1.2694(5)	0.10142(24)	6.9	0.4240(5)	0.6448(5)	0.3901(3)	6.9
1C(62)	0.0254(5)	1.3001(4)	0.27093(24)	6.0	0.4550(5)	0.6192(5)	0.2228(3)	6.6

Table 2 (Continued)

	triclinic				monoclinic			
atom	*x*	*y*	*z*	B_{eq}[b]	*x*	*y*	*z*	B_{eq}[b]
1C(72)	0.1822(6)	1.0929(5)	0.45064(25)	7.2	0.3296(7)	0.8234(7)	0.0254(5)	9.3
1C(82)	0.4605(5)	0.8652(6)	0.48367(28)	7.5	0.3322(6)	1.0734(7)	−0.0016(5)	10.1
2C(12)	0.4516(6)	0.1472(5)	0.34328(25)	6.5	0.1874(5)	1.3962(5)	0.1730(4)	6.8
2C(22)	0.3862(5)	0.1546(4)	0.17859(24)	6.1	0.1613(5)	1.3613(6)	0.3403(3)	6.8
2C(32)	0.2452(6)	0.5756(5)	0.01204(24)	6.8	0.1389(6)	1.0678(6)	0.4779(4)	7.8
2C(42)	−0.0412(5)	0.8282(5)	0.04660(23)	6.2	0.1478(5)	0.8034(5)	0.4417(3)	6.0
2C(52)	−0.2551(5)	1.0142(4)	0.21752(23)	5.7	0.1666(5)	0.6076(5)	0.2752(3)	6.4
2C(62)	−0.2023(5)	1.0191(5)	0.38545(23)	6.4	0.1967(5)	0.6424(5)	0.1050(3)	6.1
2C(72)	0.0134(5)	0.6169(4)	0.55204(19)	5.3	0.0685(5)	0.9392(5)	−0.0612(3)	6.2
2C(82)	0.2877(5)	0.3744(4)	0.51732(21)	5.3	0.0646(5)	1.1982(4)	−0.0272(3)	5.3

[a] Estimated standard deviations of the least significant digits are given in parentheses. [b] $B_{eq} = 4[V^2 \det(\beta_{ij})]^{1/2}$.

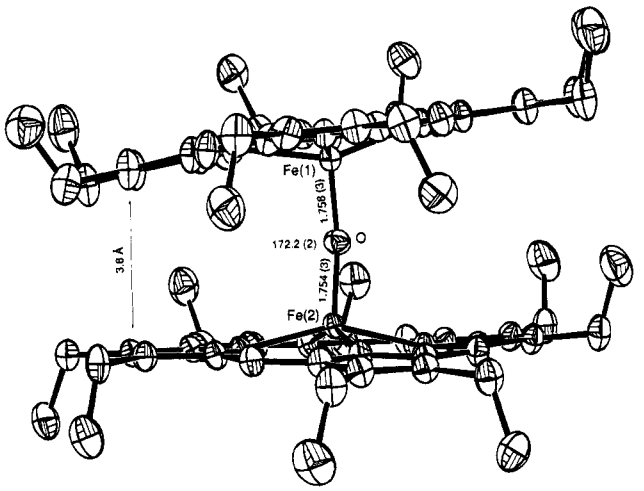

Figure 1. ORTEP diagram of the structure of triclinic $[Fe(OEP)]_2O$. Thermal ellipsoids are drawn at the 35% probability level. Porphyrin hydrogen atoms are omitted for clarity. The Fe−O−Fe bridge is in the plane of the paper.

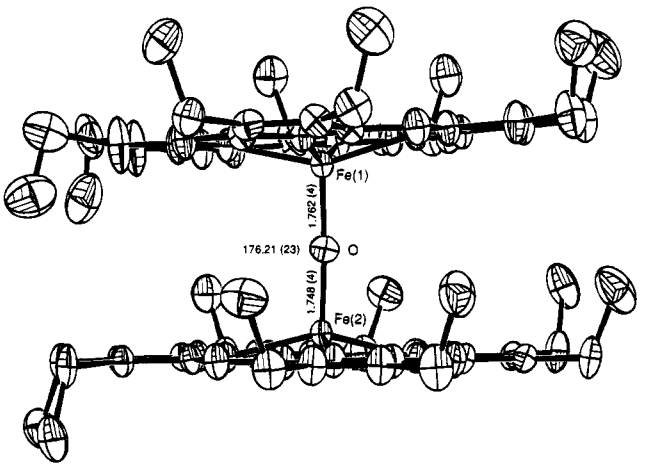

Figure 3. ORTEP diagram of the structure of monoclinic $[Fe(OEP)]_2O$. Thermal ellipsoids are drawn at the 35% probability level. Porphyrin hydrogen atoms are omitted for clarity. The Fe−O−Fe bridge is in the plane of the paper.

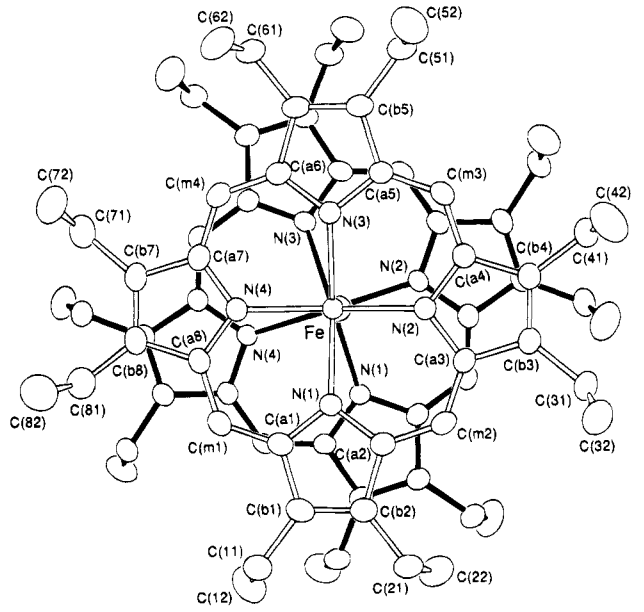

Figure 2. "Topview" of triclinic $[Fe(OEP)]_2O$ with the Fe(1)···Fe(2) axis perpendicular to the plane of the paper. Thermal ellipsoids are drawn at the 40% probability level. Porphyrin ring 2 is drawn with solid bonds while ring 1 is drawn with open bonds. Atom labels of ring 2 are identical to those shown for ring 1 following a clockwise rotation of 17°.

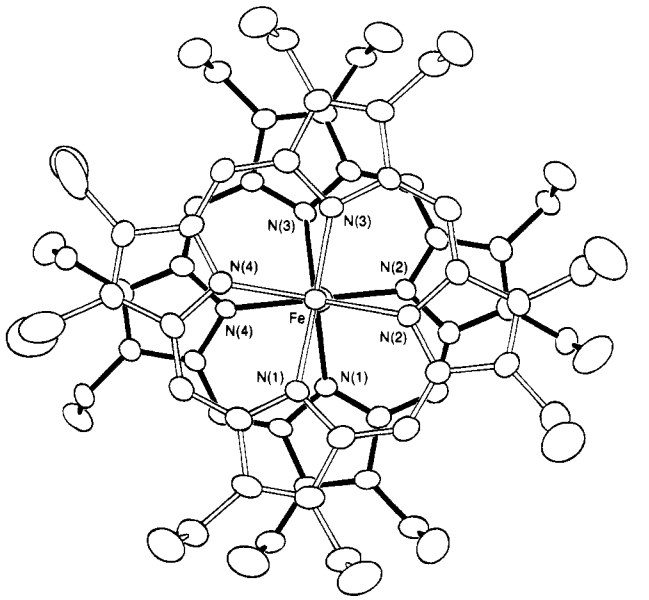

Figure 4. "Topview" of monoclinic $[Fe(OEP)]_2O$ with the Fe(1)···Fe(2) axis perpendicular to the plane of the paper. Thermal ellipsoids are drawn at the 40% probability level. Porphyrin ring 2 is drawn with solid bonds while ring 1 is drawn with open bonds. Atom labels of ring 2 are identical to those shown for ring 1 following a clockwise rotation of 16.8°.

"2". Figures 3 and 4 are the equivalent ORTEP diagrams monoclinic $[Fe(OEP)]_2O$. Individual bond distances and bond angles for triclinic $[Fe(OEP)]_2O$ are given in Tables 3 and 4, respectively; those for monoclinic $[Fe(OEP)]_2O$ are included as supplementary material. Also listed in these tables are the calculated values from the molecular mechanics calculations. Averaged values for the unique chemical classes of distances

Table 3. X-ray and MM Calculated Bond Lengths (Å) for $[Fe(OEP)]_2O$ (Triclinic Form)[a]

bond	X-ray	calc	bond	X-ray	calc
Fe(1)−O	1.758(3)	1.757	Fe(2)−O	1.754(3)	1.757
Fe(1)−1N(1)	2.074(3)	2.080	Fe(2)−2N(1)	2.079(3)	2.073
Fe(1)−1N(2)	2.078(3)	2.070	Fe(2)−2N(2)	2.075(3)	2.078
Fe(1)−1N(3)	2.074(3)	2.073	Fe(2)−2N(3)	2.076(3)	2.082
Fe(1)−1N(4)	2.077(3)	2.070	Fe(2)−2N(4)	2.084(3)	2.075
1N(1)−1C(a1)	1.371(4)	1.383	2N(1)−2C(a1)	1.373(4)	1.382
1N(1)−1C(a2)	1.373(4)	1.383	2N(1)−2C(a2)	1.373(4)	1.381
1N(2)−1C(a3)	1.378(4)	1.383	2N(2)−2C(a3)	1.373(4)	1.381
1N(2)−1C(a4)	1.371(4)	1.381	2N(2)−2C(a4)	1.370(4)	1.382
1N(3)−1C(a5)	1.374(4)	1.381	2N(3)−2C(a5)	1.373(4)	1.383
1N(3)−1C(a6)	1.371(4)	1.382	2N(3)−2C(a6)	1.376(4)	1.382
1N(4)−1C(a7)	1.369(5)	1.380	2N(4)−2C(a7)	1.367(4)	1.381
1N(4)−1C(a8)	1.360(5)	1.382	2N(4)−2C(a8)	1.366(4)	1.383
1C(a1)−1C(b1)	1.454(5)	1.451	2C(a1)−2C(b1)	1.452(5)	1.451
1C(a2)−1C(b2)	1.440(5)	1.452	2C(a2)−2C(b2)	1.446(5)	1.449
1C(a3)−1C(b3)	1.444(5)	1.450	2C(a3)−2C(b3)	1.441(5)	1.449
1C(a4)−1C(b4)	1.448(5)	1.449	2C(a4)−2C(b4)	1.444(5)	1.451
1C(a5)−1C(b5)	1.459(5)	1.449	2C(a5)−2C(b5)	1.436(5)	1.449
1C(a6)−1C(b6)	1.442(5)	1.450	2C(a6)−2C(b6)	1.448(5)	1.451
1C(a7)−1C(b7)	1.447(5)	1.447	2C(a7)−2C(b7)	1.451(5)	1.449
1C(a8)−1C(b8)	1.453(5)	1.448	2C(a8)−2C(b8)	1.448(5)	1.447
1C(a1)−1C(m1)	1.382(5)	1.373	2C(a1)−2C(m1)	1.383(5)	1.373
1C(a2)−1C(m2)	1.374(5)	1.374	2C(a2)−2C(m2)	1.388(5)	1.374
1C(a3)−1C(m2)	1.382(5)	1.375	2C(a3)−2C(m2)	1.380(5)	1.373
1C(a4)−1C(m3)	1.380(5)	1.375	2C(a4)−2C(m3)	1.377(5)	1.373
1C(a5)−1C(m3)	1.376(5)	1.375	2C(a5)−2C(m3)	1.383(5)	1.372
1C(a6)−1C(m4)	1.374(5)	1.372	2C(a6)−2C(m4)	1.380(5)	1.373
1C(a7)−1C(m4)	1.379(5)	1.373	2C(a7)−2C(m4)	1.382(5)	1.374
1C(a8)−1C(m1)	1.385(5)	1.324	2C(a8)−2C(m1)	1.387(5)	1.373
1C(b1)−1C(b2)	1.356(6)	1.351	2C(b1)−2C(b2)	1.352(5)	1.351
1C(b3)−1C(b4)	1.353(5)	1.353	2C(b3)−2C(b4)	1.350(5)	1.351
1C(b5)−1C(b6)	1.356(5)	1.351	2C(b5)−2C(b6)	1.365(5)	1.351
1C(b7)−1C(b8)	1.348(6)	1.352	2C(b7)−2C(b8)	1.366(5)	1.352
1C(b1)−1C(11)	1.510(6)	1.497	2C(b1)−2C(11)	1.502(5)	1.497
1C(b2)−1C(21)	1.511(5)	1.499	2C(b2)−2C(21)	1.503(5)	1.494
1C(b3)−1C(31)	1.502(6)	1.497	2C(b3)−2C(31)	1.500(5)	1.496
1C(b4)−1C(41)	1.506(6)	1.494	2C(b4)−2C(41)	1.502(5)	1.496
1C(b5)−1C(51)	1.503(6)	1.494	2C(b5)−2C(51)	1.498(5)	1.500
1C(b6)−1C(61)	1.512(5)	1.497	2C(b6)−2C(61)	1.491(5)	1.496
1C(b7)−1C(71)	1.531(6)	1.493	2C(b7)−2C(71)	1.501(5)	1.496
1C(b8)−1C(81)	1.538(6)	1.495	2C(b8)−2C(81)	1.492(5)	1.494
1C(11)−1C(12)	1.477(8)	1.509	2C(11)−2C(12)	1.484(7)	1.512
1C(21)−1C(22)	1.494(7)	1.514	2C(21)−2C(22)	1.504(7)	1.515
1C(31)−1C(32)	1.462(8)	1.514	2C(31)−2C(32)	1.496(8)	1.512
1C(41)−1C(42)	1.471(8)	1.504	2C(41)−2C(42)	1.502(7)	1.510
1C(51)−1C(52)	1.452(8)	1.514	2C(51)−2C(52)	1.499(7)	1.513
1C(61)−1C(62)	1.497(7)	1.512	2C(61)−2C(62)	1.499(7)	1.510
1C(71)−1C(72)	1.476(8)	1.515	2C(71)−2C(72)	1.500(6)	1.509
1C(81)−1C(82)	1.439(8)	1.507	2C(81)−2C(82)	1.501(7)	1.515

[a] Numbers in parentheses are estimated standard deviations.

and angles in the porphinato cores of the two structures are entered on their mean plane diagrams given in Figures 5 and 6. These figures also show the perpendicular displacement of each atom (in units of 0.01 Å) from the mean plane of the 24-atom core.

The structures of the $[Fe(OEP)]_2O$ molecule in the two different crystalline forms are quite similar in all important respects. The eight $Fe-N_p$ bond distances have average values of 2.077(3) Å in the triclinic form and 2.080(5) Å in the monoclinic form. The averaged axial Fe−O bond lengths are 1.756(3) and 1.755(10) Å for the two structures, respectively. The averaged displacements of the iron(III) atom from the two mean porphinato cores are 0.50 Å in the triclinic form and 0.54 Å in the monoclinic form. These structural parameters are typical for five-coordinate high-spin iron(III).[13] As will be discussed later, a most striking common feature of the molecules in the two crystal systems is the inter-ring orientation. The bridging Fe(1)−O−Fe(2) angles are 172.2(2)° in the triclinic form and 176.2(2)° in the monoclinic form. The interplanar angles between the mean 24-atom planes of a molecule are 7.3 and 2.7°, respectively, and the average mean plane separations are 4.5 and 4.6 Å.

Mössbauer Spectra. Mössbauer spectra of $[Fe(OEP)]_2O$ show a quadrupole doublet with $\Delta E_q = 0.72(1)$ mm/s and an isomer shift of 0.43(1) mm/s at 4.2 K. At 120 and 200 K, quadrupole splittings ΔE_q of 0.72(1) and 0.70(1) mm/s and isomer shifts δ of 0.43(1) and 0.37(1) mm/s were obtained, respectively. These parameters are consistent with a high-spin iron(III) complex and are comparable to the (unpublished) values cited by Sams.[14]

Molecular Mechanics. Structural features calculated for the two crystalline forms of $[Fe(OEP)]_2O$ are parenthetically shown in Table 5. All calculated individual bond lengths and angles for the triclinic form are listed in Tables 3 and 4. Those for the monoclinic form are included in supplementary material. In general, the molecular mechanics calculations reproduced the structural features observed in the crystal structures (Table 5). In particular, the average displacement of the Fe(III) atoms, the average mean plane separations, and the interplanar angles between the mean planes of porphyrins were accurately calculated. Significantly, the molecular mechanics calculations also reproduced the highly eclipsed N−Fe−Fe′−N′ dihedral angles observed in the two crystal forms of $[Fe(OEP)]_2O$. To investigate the role of the pyrrole ethyl orientations in producing a smaller N−Fe−Fe′−N′ dihedral angle, ethyl orientations were adjusted in the monoclinic form of $[Fe(OEP)]_2O$ in order to minimize these interactions. Outward rotation of all ethyl groups followed by minimization increased the N−Fe−Fe′−N′ dihedral angle to 31.6°.

Discussion

In our structural study of the novel μ-hydroxo diiron(III) complex, $\{[Fe(OEP)]_2(OH)\}ClO_4$,[2] we found that the two porphyrin rings of the cation were nearly eclipsed. We thought that this unusual porphyrin orientation was likely caused by inter-ring interactions, in particular the nonbonded interactions between peripheral ethyl groups, rather than any particular electronic effect. Since $\{[Fe(OEP)]_2(OH)\}ClO_4$ can be regarded as a protonated form of $[Fe(OEP)]_2O$, we decided to investigate the question further by determining the molecular structure of $[Fe(OEP)]_2O$ and, in particular, its inter-ring orientation. The molecular inter-ring interactions in $[Fe(OEP)]_2O$ would be expected to be somewhat smaller because of the more nearly linear Fe−O−Fe bond (expected to be >170°, compared to the 146.2° value in the hydroxide complex). After our initial structure determination of triclinic $[Fe(OEP)]_2O$ had been completed, we obtained a second crystalline form, a monoclinic form. The external features of the two kinds of crystals are difficultly distinguishable; neither form contains solvent molecules of crystallization. The two forms are differentiated only by their cell constants and (different) space groups. Since the two crystal forms are thus likely to have different packing environments, we also determined the molecular structure of the second form of $[Fe(OEP)]_2O$. There is a small difference in the calculated densities, with the triclinic form having a value of 1.235 g/cm^3 and the monoclinic form a value of 1.223 g/cm^3. A slightly better packing efficiency in the triclinic crystalline form is therefore suggested.

The molecular geometries of the two forms are very similar; the main difference occurs in the orientation of the ethyl groups.

(13) Scheidt, W. R.; Reed, C. A. *Chem. Rev.* **1981**, *81*, 543.

(14) Sams, J. R.; Tsin, T. B. In *The Porphyrins*; Dolphin, D., Ed.; Academic Press: New York, 1979; Vol. 4, Chapter 9.

Table 4. X-ray and MM Calculated Bond Angles (deg) for $[Fe(OEP)]_2O$ (Triclinic Form)[a]

angle	X-ray	calc	angle	x-ray	calc
O−Fe(1)−1N(1)	102.24(13)	114.0	O−Fe(2)−2N(1)	104.01(13)	98.6
O−Fe(1)−1N(2)	105.87(13)	105.0	O−Fe(2)−2N(2)	100.04(13)	108.4
O−Fe(1)−1N(3)	104.29(13)	98.4	O−Fe(2)−2N(3)	103.50(13)	114.2
O−Fe(1)−1N(4)	100.98(14)	105.8	O−Fe(2)−2N(4)	106.22(13)	103.7
1N(1)−Fe(1)−1N(2)	87.22(13)	85.7	2N(1)−Fe(2)−2N(2)	86.69(12)	85.8
1N(1)−Fe(1)−1N(3)	153.45(12)	147.6	2N(1)−Fe(2)−2N(3)	152.46(13)	147.1
1N(1)−Fe(1)−1N(4)	86.71(13)	85.5	2N(1)−Fe(2)−2N(4)	87.16(12)	85.4
1N(2)−Fe(1)−1N(3)	86.48(12)	85.9	2N(2)−Fe(2)−2N(3)	87.21(13)	85.3
1N(2)−Fe(1)−1N(4)	153.15(13)	148.9	2N(2)−Fe(2)−2N(4)	153.73(12)	147.6
1N(3)−Fe(1)−1N(4)	87.37(12)	85.7	2N(3)−Fe(2)−2N(4)	86.53(13)	85.4
Fe(1)−1N(1)−1C(a1)	126.11(25)	126.6	Fe(2)−2N(1)−2C(a1)	126.61(23)	126.4
Fe(1)−1N(1)−1C(a2)	125.56(24)	126.4	Fe(2)−2N(1)−2C(a2)	126.11(23)	126.5
Fe(1)−1N(2)−1C(a3)	125.32(23)	126.3	Fe(2)−2N(2)−2C(a3)	125.66(24)	125.6
Fe(1)−1N(2)−1C(a4)	127.08(24)	125.5	Fe(2)−2N(2)−2C(a4)	124.81(24)	126.5
Fe(1)−1N(3)−1C(a5)	126.70(23)	125.9	Fe(2)−2N(3)−2C(a5)	125.96(24)	126.5
Fe(1)−1N(3)−1C(a6)	126.25(23)	126.4	Fe(2)−2N(3)−2C(a6)	126.82(24)	126.6
Fe(1)−1N(4)−1C(a7)	124.23(25)	125.8	Fe(2)−2N(4)−2C(a7)	126.35(22)	126.1
Fe(1)−1N(4)−1C(a8)	125.71(25)	126.2	Fe(2)−2N(4)−2C(a8)	125.75(23)	126.0
1C(a1)−1N(1)−1C(a2)	106.06(29)	105.7	2C(a1)−2N(1)−2C(a2)	106.10(28)	105.8
1C(a4)−1N(2)−1C(a3)	105.74(29)	106.0	2C(a3)−2N(2)−2C(a4)	105.79(28)	105.8
1C(a5)−1N(3)−1C(a6)	106.08(28)	105.8	2C(a5)−2N(3)−2C(a6)	105.66(29)	105.7
1C(a7)−1N(4)−1C(a8)	106.4(3)	105.9	2C(a7)−2N(4)−2C(a8)	106.26(28)	105.9
1N(1)−1C(a1)−1C(m1)	124.5(3)	125.4	2N(1)−2C(a1)−2C(m1)	124.4(3)	125.2
1N(1)−1C(a2)−1C(m2)	124.2(3)	125.5	2N(1)−2C(a2)−2C(m2)	124.3(3)	125.8
1N(2)−1C(a3)−1C(m2)	124.2(3)	125.5	2N(2)−2C(a3)−2C(m2)	123.7(3)	125.4
1N(2)−1C(a4)−1C(m3)	123.7(3)	125.4	2N(2)−2C(a4)−2C(m3)	124.6(3)	125.4
1N(3)−1C(a5)−1C(m3)	124.5(3)	125.6	2N(3)−2C(a5)−2C(m3)	124.1(3)	125.7
1N(3)−1C(a6)−1C(m4)	124.1(3)	125.2	2N(3)−2C(a6)−2C(m4)	124.1(3)	125.4
1N(4)−1C(a7)−1C(m4)	124.8(3)	125.8	2N(4)−2C(a7)−2C(m4)	124.3(3)	125.5
1N(4)−1C(a8)−1C(m1)	124.5(3)	125.5	2N(4)−2C(a8)−2C(m1)	124.8(3)	125.7
1N(1)−1C(a1)−1C(b1)	110.0(3)	110.0	2N(1)−2C(a1)−2C(b1)	110.0(3)	110.0
1N(1)−1C(a2)−1C(b2)	110.4(3)	110.1	2N(1)−2C(a2)−2C(b2)	110.1(3)	109.9
1N(2)−1C(a3)−1C(b3)	110.2(3)	109.8	2N(2)−2C(a3)−2C(b3)	110.3(3)	110.0
1N(2)−1C(a4)−1C(b4)	110.4(3)	109.8	2N(2)−2C(a4)−2C(b4)	110.1(3)	109.9
1N(3)−1C(a5)−1C(b5)	109.8(3)	109.9	2N(3)−2C(a5)−2C(b5)	111.0(3)	110.2
1N(3)−1C(a6)−1C(b6)	110.6(3)	110.0	2N(3)−2C(a6)−2C(b6)	110.0(3)	110.0
1N(4)−1C(a7)−1C(b7)	110.1(3)	109.9	2N(4)−2C(a7)−2C(b7)	110.3(3)	109.9
1N(4)−1C(a8)−1C(b8)	109.9(3)	109.9	2N(4)−2C(a8)−2C(b8)	110.5(3)	109.9
1C(m1)−1C(a1)−1C(b1)	125.5(4)	124.6	2C(m1)−2C(a1)−2C(b1)	125.6(3)	124.8
1C(m2)−1C(a2)−1C(b2)	125.4(3)	124.4	2C(m2)−2C(a2)−2C(b2)	125.6(3)	124.3
1C(m2)−1C(a3)−1C(b3)	125.6(3)	124.7	2C(m2)−2C(a3)−2C(b3)	126.0(3)	124.6
1C(m3)−1C(a4)−1C(b4)	126.0(3)	124.8	2C(m3)−2C(a4)−2C(b4)	125.2(3)	124.7
1C(m3)−1C(a5)−1C(b5)	125.7(3)	124.5	2C(m3)−2C(a5)−2C(b5)	124.9(3)	124.1
1C(m4)−1C(a6)−1C(b6)	125.3(3)	124.8	2C(m4)−2C(a6)−2C(b6)	125.9(3)	124.6
1C(m4)−1C(a7)−1C(b7)	125.2(4)	124.3	2C(m4)−2C(a7)−2C(b7)	125.4(3)	124.6
1C(m1)−1C(a8)−1C(b8)	125.6(4)	124.6	2C(m1)−2C(a8)−2C(b8)	124.7(3)	124.4
1C(a1)−1C(b1)−1C(b2)	106.6(3)	107.1	2C(a1)−2C(b1)−2C(b2)	106.8(3)	107.0
1C(a2)−1C(b2)−1C(b1)	107.0(3)	107.1	2C(a2)−2C(b2)−2C(b1)	107.0(3)	107.3
1C(a3)−1C(b3)−1C(b4)	107.0(3)	107.1	2C(a3)−2C(b3)−2C(b4)	106.8(3)	107.1
1C(a4)−1C(b4)−1C(b3)	106.8(3)	107.2	2C(a4)−2C(b4)−2C(b3)	107.0(3)	107.1
1C(a5)−1C(b5)−1C(b6)	106.6(3)	107.2	2C(a5)−2C(b5)−2C(b6)	106.4(3)	107.0
1C(a6)−1C(b6)−1C(b5)	106.8(3)	107.0	2C(a6)−2C(b6)−2C(b5)	106.9(3)	107.2
1C(a7)−1C(b7)−1C(b8)	106.7(4)	107.2	2C(a7)−2C(b7)−2C(b8)	106.5(3)	107.0
1C(a8)−1C(b8)−1C(b7)	106.9(4)	107.0	2C(a8)−2C(b8)−2C(b7)	106.5(3)	107.2
1C(b2)−1C(b1)−1C(11)	127.9(4)	126.5	2C(b2)−2C(b1)−2C(11)	128.5(3)	126.6
1C(b1)−1C(b2)−1C(21)	128.1(4)	126.8	2C(b1)−2C(b2)−2C(21)	127.8(3)	127.0
1C(b4)−1C(b3)−1C(31)	128.3(4)	126.9	2C(b4)−2C(b3)−2C(31)	127.8(3)	126.9
1C(b3)−1C(b4)−1C(41)	127.1(4)	126.8	2C(b3)−2C(b4)−2C(41)	128.7(4)	126.7
1C(b6)−1C(b5)−1C(51)	127.9(4)	127.0	2C(b6)−2C(b5)−2C(51)	128.7(4)	126.8
1C(b5)−1C(b6)−1C(61)	128.0(4)	126.6	2C(b5)−2C(b6)−2C(61)	127.0(3)	126.5
1C(b8)−1C(b7)−1C(71)	128.6(4)	127.2	2C(b8)−2C(b7)−2C(71)	127.4(3)	126.7
1C(b7)−1C(b8)−1C(81)	126.9(4)	126.9	2C(b7)−2C(b8)−2C(81)	128.4(3)	127.0
1C(a1)−1C(b1)−1C(11)	125.5(4)	126.4	2C(a1)−2C(b1)−2C(11)	124.7(3)	126.4
1C(a2)−1C(b2)−1C(21)	124.8(4)	126.1	2C(a2)−2C(b2)−2C(21)	125.1(3)	125.8
1C(a3)−1C(b3)−1C(31)	124.7(4)	126.0	2C(a3)−2C(b3)−2C(31)	125.2(3)	126.0
1C(a4)−1C(b4)−1C(41)	126.1(4)	125.9	2C(a4)−2C(b4)−2C(41)	124.2(4)	126.2
1C(a5)−1C(b5)−1C(51)	125.5(4)	125.8	2C(a5)−2C(b5)−2C(51)	124.9(4)	126.2
1C(a6)−1C(b6)−1C(61)	125.1(4)	126.4	2C(a6)−2C(b6)−2C(61)	126.1(3)	126.3
1C(a7)−1C(b7)−1C(71)	124.6(4)	125.6	2C(a7)−2C(b7)−2C(71)	126.1(3)	126.2
1C(a8)−1C(b8)−1C(81)	126.1(4)	126.1	2C(a8)−2C(b8)−2C(81)	125.1(3)	125.8
1C(a1)−1C(m1)−1C(a8)	126.8(4)	124.9	2C(a1)−2C(m1)−2C(a8)	127.1(3)	124.8
1C(a2)−1C(m2)−1C(a3)	127.8(3)	124.9	2C(a2)−2C(m2)−2C(a3)	127.4(3)	125.0
1C(a4)−1C(m3)−1C(a5)	127.5(3)	125.0	2C(a4)−2C(m3)−2C(a5)	127.4(3)	124.9
1C(a6)−1C(m4)−1C(a7)	127.6(3)	124.9	2C(a6)−2C(m4)−2C(a7)	127.4(3)	125.0
1C(b1)−1C(11)−1C(12)	112.5(4)	112.2	2C(b1)−2C(11)−2C(12)	113.9(4)	113.0

Table 4 (Continued)

angle	X-ray	calc	angle	x-ray	calc
1C(b2)−1C(21)−1C(22)	111.9(4)	112.0	2C(b2)−2C(21)−2C(22)	112.5(4)	112.6
1C(b3)−1C(31)−1C(32)	113.5(5)	113.1	2C(b3)−2C(31)−2C(32)	113.8(4)	111.7
1C(b4)−1C(41)−1C(42)	114.3(5)	112.7	2C(b4)−2C(41)−2C(42)	112.2(4)	112.8
1C(b5)−1C(51)−1C(52)	111.8(5)	112.5	2C(b5)−2C(51)−2C(52)	112.6(4)	112.8
1C(b6)−1C(61)−1C(62)	113.0(4)	112.7	2C(b6)−2C(61)−2C(62)	113.7(4)	111.8
1C(b7)−1C(71)−1C(72)	111.1(5)	112.9	2C(b7)−2C(71)−2C(72)	114.2(4)	112.6
1C(b8)−1C(81)−1C(82)	109.7(5)	112.5	2C(b8)−2C(81)−2C(82)	113.1(4)	112.6
Fe(2)−O−Fe(1)	172.16(17)	168.0			

[a] Numbers in parentheses are estimated standard deviations.

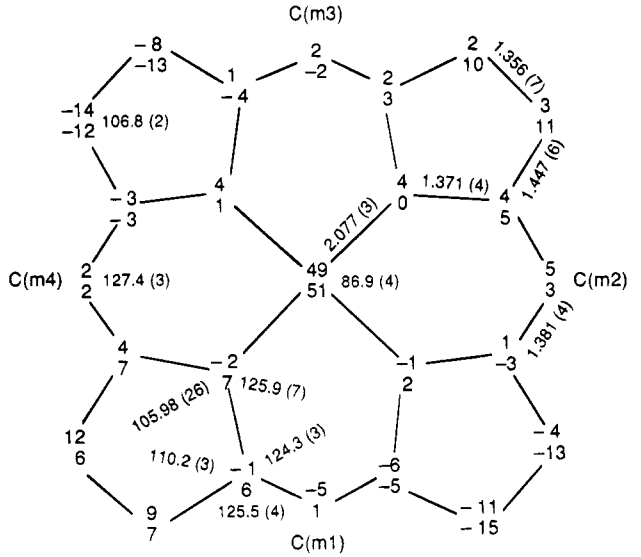

Figure 5. Formal diagram of the porphinato core of triclinic $[Fe(OEP)]_2O$, displaying the average values for the bond parameters. The numbers in parentheses are the estimated standard deviations calculated on the assumption that the averaged values were all drawn from the same population. Also displayed are the perpendicular displacements, in units of 0.01 Å, of each atom from the 24-atom mean plane of the core; the upper value of the pair is for ring 1 while the lower value is for ring 2.

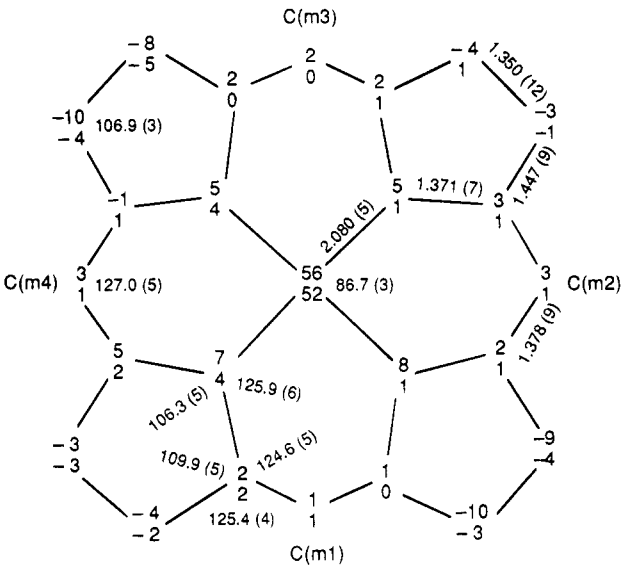

Figure 6. Formal diagram of the porphinato core of $[Fe(OEP)]_2O$ (monoclinic), displaying the averaged values for the bond parameters. The numbers in parentheses are the estimated standard deviations calculated on the assumption that the averaged values were all drawn from the same population. Also displayed are the perpendicular displacements, in units of 0.01 Å, of each atom from the 24-atom mean plane of the core; the upper value of the pair is for ring 1 while the lower value is for ring 2.

Relative (inward/outward) orientations of the ethyl groups can be seen in Figures 1 and 3. Surprisingly perhaps, the less dense monoclinic form has a total of eight ethyl groups pointing outward and eight pointing inward (between the two rings) while the denser triclinic form has ten ethyl groups pointing outward and six pointing inward. The relative orientations of the two porphyrin rings within the molecules are seen in Figures 2 and 4. One relatively easily compared measure of ring-ring orientation is that given by the averaged value of the N−Fe−Fe′−N′ dihedral (twist) angle; some dispersion in the values will arise if the two rings are not exactly parallel. These averaged values are 17.0(10) and 16.8(6)° in the triclinic and monoclinic forms, respectively; the calculated esd's give a measure of the dispersion in the individual values. Another interesting difference in the conformation of the two forms is that in the monoclinic form all of the pyrrole rings bend back from the mean porphinato planes so as to increase the interplanar separation while the triclinic form two pyrrole rings bend toward each other to yield a local separation of ~3.8 Å. These features are clearly evident in the edge-on views of the two molecules given in Figures 1 and 3. These figures and Figures 2 and 4 also show that one peripheral ethyl group on one pyrrole ring generally "interdigitates" with the two ethyl groups on the closest pyrrole ring of the other porphyrin. The only pair of pyrrole rings where this does not occur is the one in the triclinic form where the inter-ring spacing is ~3.8 Å; in this pyrrole ring pair, all four ethyl groups are oriented away from each other. We interpret all of these structural data as attesting to the importance of intramolecular inter-ring ethyl group interactions in defining the orientation.

Table 5. Crystallographic and Calculated Structural Parameters for $[Fe(OEP)]_2O$

	triclinic[a]	monoclinic[a]	"all up"[b]
Fe−Np, Å	2.077 (2.075)	2.080 (2.080)	(2.073)
Fe−O, Å	1.756 (1.757)	1.755 (1.753)	(1.741)
Δ_{av},[c] Å	0.50 (0.52)	0.54 (0.59)	(0.56)
Fe−O−Fe, deg	172.2 (168.0)	176.2 (172.2)	(155.2)
twist angle,[d] deg	17.0 (18.7)	16.8 (8.8)	(32.2)
tilt,[e] deg	7.3 (8.5)	2.7 (2.0)	(17.2)
av sepn,[f] Å	4.5 (4.5)	4.6 (4.7)	(4.7)

[a] Values in parentheses are from molecular mechanics calculation. [b] Calculated structural parameters for the hypothetical species with all ethyl groups pointing outward. [c] The average displacement of the metal centers from the 24-atom cores. [d] Average value of the four N−Fe−Fe′−N′ dihedral angles. [e] The interplanar angle between the two mean planes of the porphyrin dimer. [f] The average mean plane separation for the two porphyrin cores of the dimer.

The molecular mechanics calculations also support the importance of the interdigitation of the ethyl groups. The calculated value of the N−Fe−Fe′−N′ dihedral angle is larger in the triclinic form, where four ethyl groups point inward, compared to the monoclinic form, where six ethyl groups point between the two rings (Table 5). When the structure is idealized so that there are no ethyl groups in the space between the two

Table 6. Selected Structural Features for Monobridged Binuclear Porphinato or Phthalocyaninato Complexes

compound	M−N_p,[a] Å	M−Y,[b] Å	M−Y−M, deg	Δ,[c] Å	mean plane sepn,[d] Å	interplanar angle,[e] deg	twist angle,[f] deg	ref
			A. *meso*-Substituted Derivatives					
$[Fe(TF_5PP)]_2O$	2.088(11)	1.775(1)	178.4(5)	0.67	4.9	1.6	43	15
$[Fe(TPP)]_2O$	2.087(3)	1.763(1)	174.5(1)	0.54	4.50	3.7	35.4	16, 17
$[Fe(TMPyP)]_2O(ClO_4)_8$	2.080(8)	1.750(2)	175.1(7)	0.47	4.43	0.4	32.4	18
$[(NCH_3TPP)Fe-O-Fe(TPP)]ClO_4$	2.066(6)	1.740(4)	165.4(3)	0.46	4.4	1.6	30.2	19
$[Fe(TPC)]_2O$	2.084(7)	1.755(11)	180.0	0.55	4.60	0.0	30.2	20
$[Fe(FF)]_2O{\cdot}H_2O$	2.075(19)	1.787(17)	161.1(4)	0.63	4.7	15.8	24	21
$[Fe(TPP)]_2N$	1.991(3)	1.661(7)	180.0	0.41	4.1	0.0	31.7	22
$[Fe(TPP)]_2C$	1.980(8)	1.675	180.0	0.36	3.87	0.0	31.7	23
$[Mn(TPP)(N_3)]_2O$	2.014(19)	1.768(4)	180.0	0.10	3.88	0.0	28.5	24
$[Mo(TPP)(O)]_2O$	2.094(3)	1.936(3)	178.63(6)	−0.01	3.85	0.0	30.4	25
$[Mo(TPP)(Cl)]_2O$	2.080(6)	1.851(6)	177.5(3)	0.08	4.01	*g*	30.4	26
$[Ru(TPP)(p\text{-}OC_6H_4CH_3)]_2O$	2.050(14)	1.789(11)	177.8(7)	0.07	3.8	2.5	27.9	27
			B. β-Substituted Derivatives					
$[Fe(ODM)]_2O$	2.065(4)	1.752(1)	178.5(6)	0.53	4.55	2.9	3.8	28
$[Fe(OEP)]_2O$ (tri)	2.077(3)	1.756(3)	172.2(2)	0.50	4.5	7.3	17.0	this work
$[Fe(OEP)]_2O$ (mono)	2.080(5)	1.755(10)	176.2(2)	0.54	4.6	2.7	16.8	this work
$[Mo(OEP)(O)]_2O$	2.111(4)	1.951(1)	180.0	−0.18	3.54	0.0	22.3	29
$[Ru(OEP)Cl]_2O$	2.038	1.793(2)	180.0	0.07	3.66	0.0	21.0	30
$[Ru(OEP)(OH)]_2O$	2.067(14)	1.847(13)	180.0	0.01	3.7	0.0	22.7	31
$[Os(OEP)(OCH_3)]_2O$	2.033(28)	1.808(3)	178.4(15)	0.07	3.7	2.9	23(1)	32
$[Fe(ProtoMe_2)]_2O$	2.08	1.73	172.5	0.42	4.40	5.4	28	33
$[Mn(Pc)(Py)]_2O$	1.96(1)	1.71(1)	178	0.0	3.4	1.3	41	34
$[Fe(Pc)(1\text{-}MeIm)]_2C$	1.92(2)	1.70(1)	178(1)	0.02	3.4	1.1	45	35
$[Fe(Pc)(1\text{-}MeIm)]_2O$	1.92(3)	1.749(1)	175.1	0.02	3.5	1.5	45	36
$[Fe(TPrPc)]_2O$	2.052	1.770	145.3	0.84	4.7	36.5	31	37
$[Fe(TBuPc)]_2O$	2.056	1.748	178.5	0.61	4.7	0.9	39	37

[a] N_p refers to the pyrrole nitrogen atom in the porphyrin, phthalocyanine or porphycene. [b] Y is the bridging ligand. [c] The average displacement of the metal centers from the mean 24-atom cores. A positive value indicates that the metal is displaced toward ring center. [d] For those molecules in which the two cores are not parallel as required by crystallographic symmetry, the average separation of the individual atom from the other 24-atom core is given. [e] The dihedral angle of two mean planes of the 24-atom cores within a dimeric molecule. [f] Average of the four N−M−M′−N′ dihedral angles. [g] Information not available in the original publication, and atomic coordinates unavailable.

porphyrin rings, the calculated value of the N−Fe−Fe′−N′ dihedral angle increases to 31.6°. Other changes are related to a predicted decrease in the Fe−O−Fe′ angle caused by the decreased ethyl group interactions. The calculated values for this idealized structure are given in Table 5.

Further experimental evidence that the inter-ring orientation originates in peripheral group interactions comes from the data listed in Table 6. Listed are structural parameters for a number of singly bridged porphyrin, phthalocyanine and porphycene derivatives. Values for five-coordinate tetraarylporphyrin oxo-bridged species are listed first in the table. The twist angles observed for most of these μ-oxo diiron(III) *meso*-substituted tetraarylporphyrin derivatives are 30−35°. The relatively large twist angle is surely the result of minimizing interactions between the bulky peripheral aryl groups. The two complexes with twist angles that fall outside of this range merit special notice. An example in which this angle is smaller is $[Fe(FF)]_2O$ (24°). In this "clam shell" derivative, the porphyrin rings are linked by a urea bridge between two opposed phenyl rings and the inter-ring orientation is surely modulated by this covalent link. Indeed, it might be expected that the twist angle should be even smaller (although part of the induced strain might be relieved by the unusual nonlinear Fe−O−Fe link). In $[Fe(TF_5PP)]_2O$, in which the peripheral *meso* groups are bulkier perfluorophenyl substituents, the twist angle increases to 43°, close to the 45° maximum value. The other bridged tetraarylporphyrin derivatives either are six-coordination species or

(15) Gold, A.; Jayaraj, K.; Doppelt, P.; Fischer, J.; Weiss, R. *Inorg. Chim. Acta* **1988**, *150*, 177.
(16) Hoffman, A. B.; Collins, D. M.; Day, V. W.; Fleischer, E. B.; Srivastava, T. S.; Hoard, J. L. *J. Am. Chem. Soc.* **1972**, *94*, 3620.
(17) Swepston, P. N.; Ibers, J. A. *Acta Crystallogr., Sect. C* **1985**, *C41*, 671.
(18) Ivanca, M. A.; Lappin, A. G.; Scheidt, W. R. *Inorg. Chem.* **1991**, *30*, 711.
(19) Bartczak, T. J.; Latos-Grazynski, L.; Wyslouch, A. *Inorg. Chim. Acta* **1990**, *171*, 205.
(20) Strauss, S. H.; Pawlik, M. J.; Skowyra, J.; Kennedy, J. R.; Anderson, O. P.; Spartalian, K.; Dye, J. L. *Inorg. Chem.* **1987**, *26*, 724.
(21) Landrum, J. T.; Grimmett, D.; Haller, K. J.; Scheidt, W. R.; Reed, C. A. *J. Am. Chem. Soc.* **1981**, *103*, 2640.
(22) Scheidt, W. R.; Summerville, D. A.; Cohen, I. A. *J. Am. Chem. Soc.* **1976**, *98*, 6623.
(23) Goedken, V. L.; Deakin, M. R.; Bottomley, L. A. *J. Chem. Soc., Chem. Commun.* **1982**, 607.
(24) (a) Schardt, B. C.; Hollander, F. J.; Hill, C. L. *J. Chem. Soc., Chem. Commun.* **1981**, 765. (b) Schardt, B. C.; Hollander, F. J.; Hill, C. L. *J. Am. Chem. Soc.* **1982**, *104*, 3964.
(25) (a) Johnson, J. F.; Scheidt, W. R. *J. Am. Chem. Soc.* **1977**, *99*, 294. (b) Johnson, J. F.; Scheidt, W. R. *Inorg. Chem.* **1978**, *17*, 1280.
(26) Colin, J.; Chevrier, B.; De Cian, A.; Weiss, R. *Angew Chem., Int. Ed. Engl.* **1983**, *22*, 247.
(27) Collman, J. P.; Barnes, C. E.; Brothers, P. J.; Collins, T. J.; Ozawa, T.; Gallucci, J. C.; Ibers, J. A. *J. Am. Chem. Soc.* **1984**, *106*, 5151.
(28) Lay, K. L.; Buchler, J. W.; Kenny, J. E.; Scheidt, W. R. *Inorg. Chim. Acta* **1986**, *123*, 91.
(29) Kim, K.; Sparapany, J. W.; Ibers, J. *Acta Crystallogr., Sect. C* **1987**, *C43*, 2076.
(30) Masuda, H.; Taga, T.; Osaki, K.; Sugimoto, H.; Mori, M.; Ogoshi, H. *Bull. Chem. Soc. Jpn.* **1982**, *55*, 3887.
(31) Masuda, H.; Taga, T.; Osaki, K.; Sugimoto, H.; Mori, M.; Ogoshi, H. *J. Am. Chem. Soc.* **1981**, *103*, 2199.
(32) Masuda, H.; Taga, T.; Osaki, K.; Sugimoto, H.; Mori, M. *Bull. Chem. Soc. Jpn.* **1984**, *57*, 2345.
(33) (a) Radonovich, L. J.; Caughey, W. S.; Hoard, J. L. Unpublished results (personal communication from J. L. Hoard). (b) Anderson et al. have obtained essentially similar results: Anderson, O. P.; Schauer, C. K.; Caughey, W. S. *J. Am. Crystallogr. Assoc., Ser. 2* **1982**, *10*, 23.
(34) Vogt, L. H.; Zalkin, A.; Templeton, D. H. *Inorg. Chem.* **1967**, *6*, 1725.
(35) Rossi, G.; Goedken, V. L.; Ercolani, C. *J. Chem. Soc., Chem. Commun.* **1988**, 46.
(36) Ercolani, C.; Monacelli, F.; Dzugan, S.; Goedken, V. L.; Pennesi, G.; Rossi, G. *J. Chem. Soc., Dalton Trans.* **1991**, 1309.
(37) Lausmann, M.; Zimmer, I.; Lex, J.; Lueken, H.; Wieghardt, K.; Vogel, E. *Angew. Chem., Int. Ed. Engl.* **1994**, *33*, 736.

have a different bridging ligand (N,C). Nonetheless, the remaining *meso*-substituted compounds listed in Table 6 are also seen to hold to this twist angle pattern.

Table 6 also lists values of the twist angles for a second series of μ-oxo bridged derivatives, those which have peripheral β-substituents. All derivatives with only ethyl groups at the periphery are seen to have twist angles in the range 17−23°, significantly smaller than those of the *meso*-substituted derivatives. Although the twist angle is apparently unaffected by the mean plane separation (range is 3.5−4.5 Å), there is an interesting effect on the ethyl group orientations. In the μ-oxo diiron(III) derivatives, with interplanar separations of about 4.5 Å, about half of the methyl carbons of the ethyl groups point between the two rings and the close C···C nonbonded distances between ethyl carbon atoms are ~3.7 Å. In these compounds the contacts are between methylene and methyl carbon atoms. Four other bridged derivatives, with interplanar separations of 3.5−3.7 Å, have all ethyl groups pointing away from the center of the two rings. Nonetheless, the shortest C···C nonbonded distances between ethyl carbon atoms remains ~3.7 Å; however, the closest contacts are now between pairs of methylene carbon atoms.

Again, derivatives that fall outside the general range are informative. The derivative $[Fe(ODM)]_2O$ has almost exactly eclipsed porphyrin rings. Each porphyrin ring in this compound has, in addition to eight pyrrole β-ethyl groups, two opposite *meso*-methyl groups. The addition of two additional peripheral groups leads to substantial steric crowding at the periphery, consequent core ruffling and near-eclipsed rings in order to minimize the intra- and inter-ring interactions. (The *meso*-methyl groups of opposite porphyrin rings are 86° apart.) The phthalocyanine derivatives (in which the formal β-substituents lie in the samee plane as the macrocycle) have a fully staggered orientation (twist angle of 45°). It is a reasonable presumption that the staggered orientation results from the macrocyclic atoms alone.

The final two entries in Table 6 also shows the importance of peripheral group interactions. In these two porphycene derivatives,[37] there are four peripheral groups which are either *n*-propyl or *tert*-butyl. The derivative with the less sterically demanding *n*-propyl groups is seen to have a somewhat smaller inter-ring orientation as well as a significantly smaller Fe−O−Fe angle, as expected for the differing steric requirements.

Structural features of the iron(III) coordination group in the two forms of $[Fe(OEP)]_2O$ are quite similar to those of the other μ-oxo derivatives listed in Table 6. This table lists four structural parameters: the average equatorial Fe−N_p bond length, the axial Fe−O bond length, the Fe−O−Fe bridge angle and Δ, the displacement of the iron from the mean plane of the macrocycle. The coordination group data do not suggest that either of the $[Fe(OEP)]_2O$ derivatives are unusual in any way.

Acknowledgment. We thank the National Institutes of Health for support of this research under Grants GM-38401 to W.R.S. and GM-16406 to P.G.D. Funds for the purchase of the FAST area detector diffractometer was provided through NIH Grant RR-06709 to the University of Notre Dame. Work performed at Sandia National Laboratory was supported by the U.S. Department of Energy (Contract DE-AC04-94ALB5000). We thank Professor Emanuel Vogel and Dr. Johann Lex for providing atomic coordinates for the porphycene derivatives.

Supplementary Material Available: Table S1, giving complete crystallographic details for $[Fe(OEP)]_2O$, Tables S2 and S3, listing anisotropic thermal parameters and fixed hydrogen atom coordinates for $[Fe(OEP)]_2O$ in the triclinic system, Tables S4−S7, listing bond lengths and angles, anisotropic thermal parameters, and fixed hydrogen atom coordinates for monoclinic $[Fe(OEP)]_2O$, and Table S8, giving the parameters for the potential energy terms of Fe−O stretch and Fe−O−Fe angle bend (16 pages). Ordering information is given on any current masthead page.